BioTechnology

An Indian Journal

FULL PAPER

Novel MC-DTC control method for induction motor based on space vector modulation

Cai Bin-jun[1,2], Nian Xiao-hong[1,*]
[1]School of Information Science and Engineering, Central South University,
Changsha 410004, (P.R.CHINA)
[2]College of Electrical & Information Engineering, Hunan Institute of Engineering,
Xiangtan 411101, (P.R.CHINA)
E-mail : xhnian@mail.csu.edu.cn

ABSTRACT

This paper presents a novel MC-DTC method for fed induction motor based on space vector modulation. The advantages of DTC method are combined with the advantages of the matrix converter based on space vector modulation technique. This proposed novel method provides a precious input power factor control capability beside the high control performances. Furthermore, Conventional principles of DTC and MC were described. The combination of the DTC and MC were given in details. The simulation and experiment research were carried out to identify the new method effectiveness. The results of induction motor control at steady state are shown to improve the low-speed performance and strong adaptability of this novel control strategy.

KEYWORDS

Matrix converter; DTC; Induction motor; Space vector modulation; Low-speed performance.

© **Trade Science Inc.**

INTRODUCTION

In two recent decades, due to the need to increase the quality and the efficiency of the power supply and usage, three phase matrix converter becomes a modern energy converter. The research of matrix converter has been carried on with many theoretical[1],[2],[3].These achievements along with the emergence of bidirectional switch make it possible to apply the matrix converter to practical applications. Various methods to control the matrix converter have been proposed [4],[5], being the scalar modulation and the indirect space vector modulation widely used. It fulfills all requirements of the conventionally used rectifier/dc link/ inverter structures. Some advantages of the matrix converter can be seen as following: the use of a compact voltage source, providing sinusoidal voltage with varying amplitude and frequency besides the sinusoidal input current and unity input power factor at power supply side. Matrix converter has a simple topology and a compact design due to the lack of dc-link capacitor for energy storage.

Since the DTC method has been proposed in the middle of 1980's, DTC method becomes one of the high performance control strategies for AC machine to provide a very fast torque and flux control[6][7]. There are no requirements for coordinate transformation, no requirements for PWM generation and current regulators. It is widely known to produce a quick and fast response in AC drives by selecting the proper voltage space vector according to the switching status of inverter which is determined by the error signal of reference flux linkage and torque with their estimated values and the position of the estimated stator flux. Some research is being done to adapt DTC to new converters and also to reduce the torque ripple, which is one of its main drawbacks. DTC is the direct control of torque and flux of a drive by the selection, through a look-up table, of the inverter voltage space vectors. The main advantage of DTC is its structure, no coordinate transformations and no PWM generation are needed. However, torque and flux modulus values and the sector of the flux are needed. Not only it is a very simple and robust signal processing scheme but also a very quick and precise torque control response is achieved.

In this paper, a novel MC-DTC method for fed induction motor based on space vector modulation is proposed. The advantages of DTC method are combined with the advantages of the matrix converter based on space vector modulation technique.The appropriate switching configurations of the matrix converter for each constant time are presented in an opportune switching table[8],[9],[10]. The table is only entered by the imaginary voltage vector, which is generated from the DTC method for voltage source inverter, and the position of input voltage vector which can be measured exactly. Simulation and experiment at the high-speed and low-speed are carried out to prove the good performances of the novel method.

CONVENTIONAL DIRECT TORQUE CONTROL

Mathematical mode of induction machine

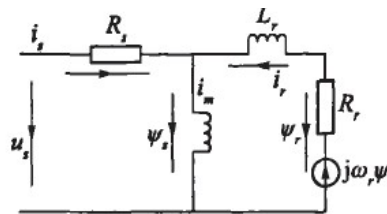The mathematical mode of induction machine is shown in Figure 1.

Figure 1 : The mathematiacal mode of induction motor

According to Figure 1 flux-linkage equations of induction machines in the stator stationary reference frame as follows.

$$\psi_{\alpha s} = \int \left(v_{\alpha s} - R_s i_{\alpha s} \right) dt \qquad (1)$$

$$\psi_{\beta s} = \int \left(v_{\beta s} - R_s i_{\beta s} \right) dt \qquad (2)$$

Where $\psi_{\alpha s}$ and $\psi_{\beta s}$ are the α-axis and β-axis component of $\overset{\mathbf{1}}{\psi}_s$ respectively; $v_{\alpha s}$ and $v_{\beta s}$ are the α-axis and β-axis component of $\overset{\mathbf{1}}{v}_s$ respectively; $i_{\alpha s}$ and $i_{\beta s}$ are the α-axis and β-axis component of $\overset{\mathbf{1}}{i}_s$.

The electromagnetic torque can be expressed using the following equation.

$$T_e = \frac{3}{2} n_p (\overset{\mathbf{1}}{\psi}_s \times \overset{\mathbf{1}}{i}_s) = \frac{3}{2} n_p (\psi_{\alpha s} i_{\beta s} - \psi_{\beta s} i_{\alpha s}) \qquad (3)$$

Where T_e is electromagnetic torque and n_p is the number of rotor pole pairs.

Principle of DTC

The basic principle in conventional DTC for induction motors is to directly select stator voltage vectors by means of a hysteresis stator flux and torque control. As it is shown in Figure 2.
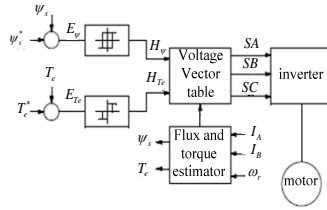

Figure 2 : The diagram block of basic DTC

From Figure 2 can obtain stator flux ψ_s^* and torque T_e^* references are compared with the corresponding estimated values. Both stator flux and torque errors, E_ψ and E_{Te}, are processed by means of a hysteresis band comparators. In particular, stator flux is controlled by a two-level hysteresis comparator, whereas the torque is controlled by a three-level comparator. On the basis of the hysteresis comparators and stator flux sector a proper VSI voltage vector is selected by means of the switching table given in Table 1.

TABLE 1 : Basic DTC switching table

Sector of Flux→		1	2	3	4	5	6
$c_\varphi = 0$	$c_T = -1$	$V_{2\text{-VSI}}$	$V_{3\text{-VSI}}$	$V_{4\text{-VSI}}$	$V_{5\text{-VSI}}$	$V_{6\text{-VSI}}$	$V_{1\text{-VSI}}$
	$c_T = 0$	$V_{7\text{-VSI}}$	$V_{0\text{-VSI}}$	$V_{7\text{-VSI}}$	$V_{0\text{-VSI}}$	$V_{7\text{-VSI}}$	$V_{0\text{-VSI}}$
	$c_T = 1$	$V_{6\text{-VSI}}$	$V_{1\text{-VSI}}$	$V_{2\text{-VSI}}$	$V_{3\text{-VSI}}$	$V_{4\text{-VSI}}$	$V_{5\text{-VSI}}$
$c_\varphi = +1$	$c_T = -1$	$V_{3\text{-VSI}}$	$V_{4\text{-VSI}}$	$V_{5\text{-VSI}}$	$V_{6\text{-VSI}}$	$V_{1\text{-VSI}}$	$V_{2\text{-VSI}}$
	$c_T = 0$	$V_{0\text{-VSI}}$	$V_{7\text{-VSI}}$	$V_{0\text{-VSI}}$	$V_{7\text{-VSI}}$	$V_{0\text{-VSI}}$	$V_{7\text{-VSI}}$
	$c_T = 1$	$V_{5\text{-VSI}}$	$V_{6\text{-VSI}}$	$V_{1\text{-VSI}}$	$V_{2\text{-VSI}}$	$V_{3\text{-VSI}}$	$V_{4\text{-VSI}}$

MC SPACE VECTOR MODULATION

Working principle of MC

MC is an AC-AC converter, with mxn bidirectional switches, which connects an m-phase voltage source to an n-phase load. The three-phase, 3x3 switches, MC shown in Figure 3 is the most interesting. It connects a three phase voltage source to a three-phase load[11].
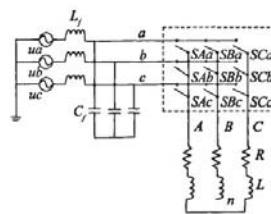

Figure 3 : The topology of matrix converter

In the MC shown in "Fig.3," $v_{si}, i = \{A, B, C\}$ are the source voltages, $i_{si}, i = \{A, B, C\}$ are the source currents. v_{jN}, $j = \{A, B, C\}$ are the load voltages, $i_j, j = \{A, B, C\}$ are the load currents, $v_i, i = \{A, B, C\}$ are the MC input voltages and i_i, $i = \{A, B, C\}$ are the input currents. A switch, $S_{ij}, i = \{A, B, C\}, j = \{a, b, c\}$ can connect phase i of the input to phase j of the load. With a suitable switching strategy, arbitrary voltages v_{jN} at arbitrary frequency can be synthesized.

Switches are characterized by the following equation.

$$S_{ij} = \begin{cases} 0 & witch \quad S_{ij} \quad is \quad open \\ 1 & witch \quad S_{ij} \quad S_{ij} \quad clos\grave{e} \end{cases} \qquad (4)$$

A mathematical model of MC can be derived from "Fig.3" as follows:

$$\begin{bmatrix} v_{aN}(t) \\ v_{bN}(t) \\ v_{cN}(t) \end{bmatrix} = \begin{bmatrix} S_{Aa}(t) & S_{Ba}(t) & S_{Ca}(t) \\ S_{Ab}(t) & S_{Bb}(t) & S_{Cb}(t) \\ S_{Ac}(t) & S_{Bc}(t) & S_{Cc}(t) \end{bmatrix} \cdot \begin{bmatrix} v_A(t) \\ v_B(t) \\ v_C(t) \end{bmatrix} \quad (5)$$

$$\begin{bmatrix} i_A(t) \\ i_B(t) \\ i_C(t) \end{bmatrix} = \begin{bmatrix} S_{Aa}(t) & S_{Ab}(t) & S_{Ac}(t) \\ S_{Ba}(t) & S_{Bb}(t) & S_{Bc}(t) \\ S_{Ca}(t) & S_{Cb}(t) & S_{Cc}(t) \end{bmatrix} \cdot \begin{bmatrix} i_a(t) \\ i_b(t) \\ i_c(t) \end{bmatrix} \quad (6)$$

The conventional three-phase to three-phase matrix converter's modulation process consists of two processes of AC-DC and DC-AC. It is shown in Figure 4.
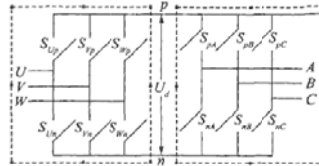

Figure 4 : The topology of 3x3 matrix converter

The control signal for bidirectional switches come from the control circuit and drive circuits. The ratio cycles of 9 bidirectional switches correspond to a 3x3 matrix in each switching period.

DC-AC converter space vector modulation

6 power switches of inverter with 8 possible combinations shown in Figure 3 are corresponding to effective voltage space vector $U_1 - U_6$ and 2 zero vector U_0, U_7. The phase angle between one effective voltage space vector and adjacent one is 60 degrees. They constitute 6 uniform segments. The three digits in brackets express the linking state between three-phase output A, B, C and the input DC, such as $M = 101$ which represents the switching of the switches S_{pA}, S_{nB}, S_{pC}.

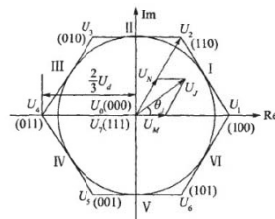The output voltage and the corresponding switching states are represented in Figure 5.

Figure 5 : The output voltage vector and switching states

Any expected output voltage space vector U_J is formed by adjacent two basic output voltage vectors U_M, U_N and zero output voltage U_0 or U_7. Suppose the angle between U_J and U_M is θ_J.

$$U_J = d_M U_M + d_N U_N + d_0 U_0 \quad (7)$$

Where d_M, d_N and d_0 are the ratio cycles of U_M, U_N and U_0 respectively. And

$$d_M = T_M / T_\delta = m_v \sin(60^0 - \theta_J) \quad (8)$$

$$d_N = T_N / T_\delta = m_v \sin \theta_J \quad (9)$$

$$d_0 = 1 - d_M - d_N \quad (10)$$

Where T_M, T_N is the switching time of vectors U_M and U_M respectively. T_δ is the switching period of PWM. m_v is the modulation index of output voltage. And

$$m_v = \left(2/3\right)^{1/2} U_{om} / \left(U_{im} m_c \cos\phi\right) \tag{11}$$

Where U_{om} and U_{im} are the amplitude of output and input voltage, m_c is the input current modulation index, generally set $m_c = 1$, ϕ is the input power factor angle.

When the rotating space vector U_J locates in a segment, the local average of output voltage can be formed by two adjacent basic voltage space vectors constituting this segment and one zero voltage space vector.

AC-DC converter space vector modulation

The space vector modulation process of AC-DC is completely similar to the modulation process of DC-AC. Its topology is represented in the left dotted line frame of "Fig.4". The corresponding formulas are similar as well. After rectification, the *DC* voltage is.

$$U_d = 1.5 m_c U_{im} \cos\varphi \tag{12}$$

MC space vector modulation

Three-phase matrix converter module includes nine bidirectional switches as shown in Figure 6. There are 27 possible switching configurations (SCs), only 21 SCs can be used to implement the DTC algorithm for MC as shown in Table 2: group I (± 1, ± 2, …, ± 9) consists of the SCs which have two output phases connected to the same one of the other input phase, group II (0_a, 0_b, 0_c) consists of the SCs which have all output phases connected to a common input phase. For each SCs, the corresponding output line-to-neutral voltage vector and input line current vector have the fixed directions as represented in Figure 6.
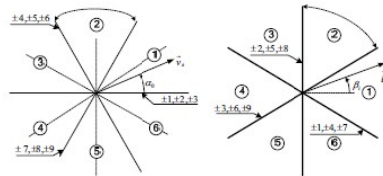

Figure 6 : (a) The output voltage; (b) The intput line current

TABLE 2 : MC active and zero vectors

Group	Vector	A B C	V_o	α_o	I_i	β_i
I	$+1_{SC}$	a b b	$2/3 v_{ab}$	0	$2/\sqrt{3} i_A$	$-\pi/6$
	-1_{SC}	b a a	$-2/3 v_{ab}$	0	$-2/\sqrt{3} i_A$	$-\pi/6$
	$+2_{SC}$	b c c	$2/3 v_{bc}$	0	$2/\sqrt{3} i_A$	$\pi/2$
	-2_{SC}	c b b	$-2/3 v_{bc}$	0	$-2/\sqrt{3} i_A$	$\pi/2$
	$+3_{SC}$	c a a	$2/3 v_{ca}$	0	$2/\sqrt{3} i_A$	$7\pi/6$
	-3_{SC}	a c c	$-2/3 v_{ca}$	0	$-2/\sqrt{3} i_A$	$7\pi/6$
	$+4_{SC}$	b a b	$2/3 v_{ab}$	$2\pi/3$	$2/\sqrt{3} i_B$	$-\pi/6$
	-4_{SC}	a b a	$-2/3 v_{ab}$	$2\pi/3$	$-2/\sqrt{3} i_B$	$-\pi/6$
	$+5_{SC}$	c b c	$2/3 v_{bc}$	$2\pi/3$	$2/\sqrt{3} i_B$	$\pi/2$
	-5_{SC}	b c b	$-2/3 v_{bc}$	$2\pi/3$	$-2/\sqrt{3} i_B$	$\pi/2$
	$+6_{SC}$	a c a	$2/3 v_{ca}$	$2\pi/3$	$2/\sqrt{3} i_B$	$7\pi/6$
	-6_{SC}	c a c	$-2/3 v_{ca}$	$2\pi/3$	$-2/\sqrt{3} i_B$	$7\pi/6$
	$+7_{SC}$	b b a	$2/3 v_{ab}$	$4\pi/3$	$2/\sqrt{3} i_C$	$-\pi/6$
	-7_{SC}	a a b	$-2/3 v_{ab}$	$4\pi/3$	$-2/\sqrt{3} i_C$	$-\pi/6$
	$+8_{SC}$	c c b	$2/3 v_{bc}$	$4\pi/3$	$2/\sqrt{3} i_C$	$\pi/2$
	-8_{SC}	b b c	$-2/3 v_{bc}$	$4\pi/3$	$-2/\sqrt{3} i_C$	$\pi/2$
	$+9_{SC}$	a a c	$2/3 v_{ca}$	$4\pi/3$	$2/\sqrt{3} i_C$	$7\pi/6$
	-9_{SC}	c c a	$-2/3 v_{ca}$	$4\pi/3$	$2/\sqrt{3} i_C$	$7\pi/6$
II	0_a	a a a	0	-	0	-
	0_b	b b b	0	-	0	-
	0_c	c c c	0	-	0	-

Novel DTC-MC based on SVM

The novel DTC-MC method will apply the direct SVM technique to overcome the disadvantages of the conventional DTC for matrix converter[12],[13]. According to the input voltage line to neutral vector sector location, to combine the desired imaginary non-zero VSI voltage vector, the two non-zero voltage vectors will be selected.

The criteria utilized to implement the switching patterns for the matrix converter can be explained referring to the following example.

We can assume the imaginary VSI voltage vector is V_1, and the input voltage lint-to-neutral vector [14],[15] is located in sector 1 as shown in Figure 7.
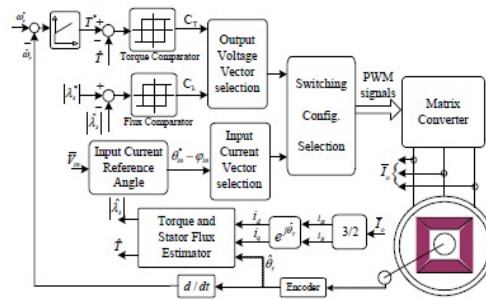

Figure 7 : Block diagram of novel DTC-MC based on SVM

From Table 2, in order to generate a voltage vector in the same direction of V_1, there are 6 possible SCs (±1, ±2, ±3). According to the input voltage vector location, there are only 3 SCs having the voltage vectors as same direction to V_1: +1, -2 and -3. To synthesize the input current vector to be in phase with the input voltage vector located in sector 1, two SCs finally selected are +1 and -3. The switching table based on these criteria is shown in Table 3.

TABLE 3 : MC-DTC switching table using SVM

Sector of V	1		2		3		4		5		6	
Duty ratio	t_1	t_2	t_1	t_2	t_1	t_2	t_1	t_2	t_1	t_2	t_1	t_2
V_{1-vsi}	+1	-3	-3	+2	+2	-1	-1	+3	+3	-2	-2	+
V_{2-vsi}	-7	+9	+9	-8	-8	+7	+7	-9	-9	+8	+8	-7
V_{3-vsi}	+4	-6	-6	+5	+5	-4	-4	+6	+6	-5	-5	+4
V_{4-vsi}	-1	+3	+3	-2	-2	+1	+1	-3	-3	+2	+2	-3
V_{5-vsi}	+7	-9	-9	+8	+8	-7	-7	+9	+9	-8	-8	+7
V_{6-vsi}	-4	+6	+6	-5	-5	+4	+4	-6	-6	-5	-5	-4

As shown in Figure 7, the output voltage of matrix converter for each SCs is calculated.

$$V_S = \begin{bmatrix} S_{aA} & S_{aB} & S_{aC} \\ S_{bA} & S_{bB} & S_{bC} \\ S_{cA} & S_{cB} & S_{cC} \end{bmatrix} \begin{bmatrix} V_a \\ V_b \\ V_c \end{bmatrix} = T \begin{bmatrix} V_a \\ V_b \\ V_c \end{bmatrix} \qquad (13)$$

Where the switching function S_{ij} is 1 when the switch joining input line i to output line J is ON and i is 0 otherwise, $i = a,b,c$ and $J=A,B,C$. Matrix T represents the status of each switching configuration in Table 2.

The input voltage vector of induction motor in the stationary reference frame for each sampling period.

$$\bar{v}_s = \begin{bmatrix} \bar{v}_{sd} \\ \bar{v}_{sq} \end{bmatrix} = \frac{2}{3} \begin{bmatrix} 1 & -\dfrac{1}{2} & -\dfrac{1}{2} \\ 0 & \dfrac{\sqrt{3}}{2} & \dfrac{\sqrt{3}}{2} \end{bmatrix} \begin{bmatrix} t_1 T_x + t_2 T_y \end{bmatrix} \begin{bmatrix} V_a \\ V_b \\ V_c \end{bmatrix} \qquad (14)$$

From Figure 6, the duty ratios of the two non-zero Scs. are calculated as follows.

$$t_1 V_x + t_2 V_y = V_{VSI}$$
$$\frac{t_1 V_x}{\sin(\pi/6 - \alpha_i)} = \frac{t_2 V_y}{\sin(\pi/6 + \alpha_i)} \qquad (15)$$
$$t_1 + t_2 = 1$$

$$t_1 = \frac{\sin\left(\pi/6 - \alpha_i\right)}{\cos\left(\alpha_i\right)}$$

$$t_2 = \frac{\sin\left(\pi/6 + \alpha_i\right)}{\cos\left(\alpha_i\right)} \qquad (16)$$

The induction motor stator flux can be obtained from the calculated input voltage and the measured stator currents.

$$\overset{\rangle}{\phi}_s = \int\left(\overline{v}_s - R_s\overline{i}_s\right)dt \qquad (17)$$

The motor estimated torque can be obtained.

$$\overset{\rangle}{T} = \frac{3n_p}{2}\left(\overset{\rangle}{\phi}_{sd}i_{sq} - \overset{\rangle}{\phi}_{sq}i_{sd}\right) \qquad (18)$$

SIMULATION OF MC-DTC BASED ON SVM

The simulation model of MC-DTC based on SVM

In order to verify the behavior of the proposed scheme, some simulation has been carried out assuming a sampling period of 50μs. The system simulation model is shown in Figure 8. The machine utilized for simulations is a three-phase $3kw$ cage induction motor:

$P_n = 2.2kw$, $U_n = 380v$, $R_s = 4.35\Omega$, $R_r = 0.43\Omega$, $L_s = 2mH$, $L_r = 2mH$, $L_m = 69.31mH$, $J = 0.089kg \cdot m^2$, $P = 2$.

The whole system has been simulated using the Simulink package. Equation (5) and Equation (6) are used to obtain the matrix output voltages and the input currents respectively, thus assuming ideal switching devices. The mains filtered line current is calculated on the basis of the matrix input current.
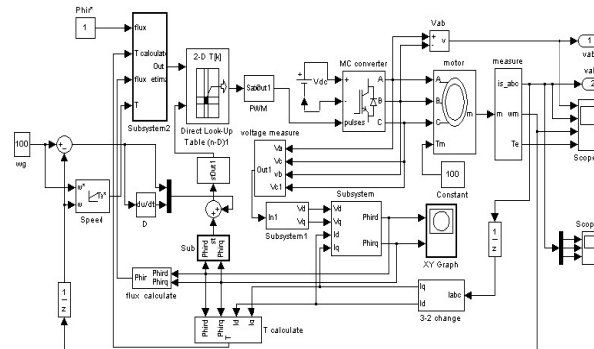

Figure 8 : The simulation model MC-DTC based on SVM

The simulation result of MC-DTC based on SVM

At the high speed operation, induction motor is running at speed $1000rpm$, rated load torque $25Nm$ and flux reference $0.6wb$. The simulation result show in Figure 9-Figure 10.

Figure 9 shows a good performance in terms of stator flux. As it can be seen in Figure 9, stator flux shows a circle waveform.
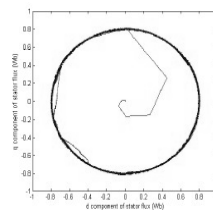

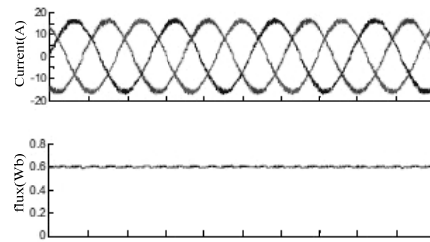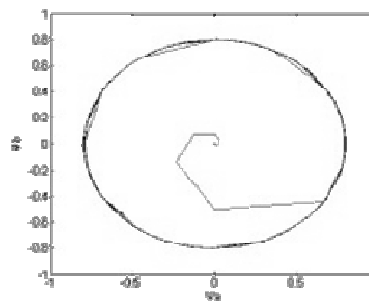**Figure 9 : Flux at** $100rpm$ **,** $25Nm$ **for MC-DTC**

Figure 10 : Current flux and torque at $1000rpm$ **for MC-DTC**

Figure 10 shows stator flux and electromagnetic torque of the induction motor fully following the reference values. Furthermore, the stator currents have sinusoidal waveforms. This figure emphasizes the good performance of the drive system with regard to the implementation of the novel MC-DTC method.

At the low speed operation, induction motor is running at a very low speed $100rpm$, load torque $20Nm$ and flux reference $0.6\,wb$. The simulation result show in Figure 11- Figure 12.

Figure 11 : Flux at $100rpm$ **,** $25Nm$ **for MC-DTC**
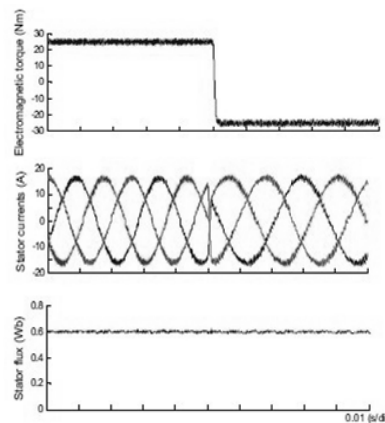
Figure 13 : Torque, current and flux at $100rpm$ **for MC-DTC**

Figure 12 shows the dynamic performances of the novel control method at the rotor speed $100rpm$ and load torque change as a step command from $+25Nm$ to $-25Nm$. The electromagnetic torque shows a very good response and the stator current waveforms are almost sinusoidal immediately right after the step command.

EXPERIMENT OF MC-DTC BASED ON SVM

The novel method had been tested. The parameters are same as simulation parameters. The motor was fed by a $7.5kw$ MC. The MC-DTC algorithms were implemented in a TMS320LF2407 DSP achieving a sample period of 50μs. The four-step commutation process, required when bidirectional switches are used, was implemented in a FPGA. A current-controlled hysteresis brake provides the load torque. A block diagram of the system setup is shown in Figure 13.
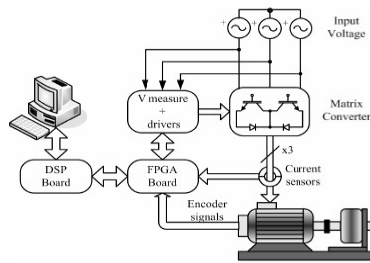
Figure 13 : The system setup of MC-DTC based on SVM

At the high speed operation, induction motor is running at speed $1000rpm$, rated load torque $0.2Nm$ and flux reference $0.6wb$. The experiment result show in Figure 14-Figure 15.
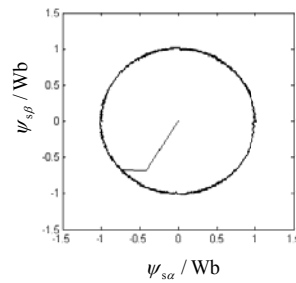

Figure 14 : The result of flux at $1000rpm$, $25Nm$ for MC-DTC

It can be seen from Figure 14-Figure 15, electromagnetic torque, stator current, and stator flux performance at high speed respectively. As regard the ripple, the proposed novel method clearly improves the performance of both the torque and flux. Furthermore, in the case of torque, the type of the applied vectors is also shown. At the same time, the inner torque hysteresis bands in the proposed method are identical to the torque hysteresis bands in the classical method. Thus, the outer bands in the proposed method can be seen as security limits above which the large vectors are used in order to quickly force the torque towards its reference value.
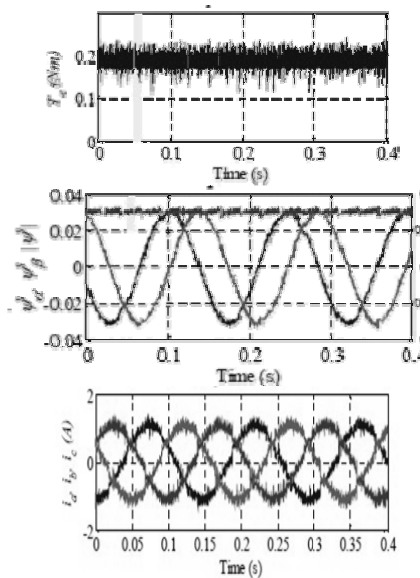

Figure 15 : During a load torque step command from $+25Nm$ to $-25Nm$ the torque, current and flux at $1000rpm$ for MC-DTC

At the low speed operation, induction motor is running at a very low speed $100rpm$, load torque $25Nm$ and flux reference $0.6wb$ 0. The experiment result show in Figure 16-Figure 17.
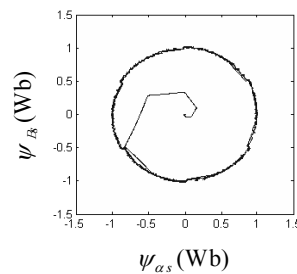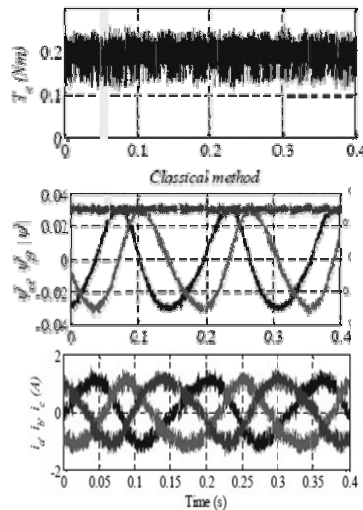
Figure 16 : The flux at $100rpm$**,** $25Nm$ **for MC-DTC**

Figure 17 : During a load torque step command from $+25Nm$ **to** $-25Nm$ **the torque,current and flux at** $100rpm$ **for MC-DTC**

Figure 16-Figure 17 show that the stator flux,torque in the low frequency range when compared with the high speed. However, this is not seen as a constraint since a re-design of the MC input filter would be enough to overcome this drawback.

In order to study the dependency of the torque ripple with respect to both the torque reference and the motor speed, several tests were carried out at low-speed. The standard deviation of the torque was calculated to measure the torque ripple.

CONCLUSION

This paper presents a new DTC-SVM method for matrix converter. The advantages of the DTC method have been successfully combined with the SVM method on matrix converter. A new switching table for the DTC-SVM which fully controls the induction motor requirements is suggested. The simulation and experiment results on the induction motor at the low and high speed range are shown to validate the effectiveness of the new control scheme. Furthermore, the novel control strategy shows the better input current harmonic spectrum and low-speed performance as compared to the conventional DTC method and it can make the flux and torque small and stable. It has advantages and good future, it is worth further studying.

ACKNOWLEDGMENTS

REFERENCES

[1] Guo yougui, Zhu jianlin，"New modulaiton strategy on raising voltage transfer ratio for matrix converter,"control theroy and applications,2006,23(4):542-546.
[2] Ding wei, Zhu jianlin, "Matrix converter and its research situation," *natural science journal of xiangtan university*, 2002,24(2):185-187.
[3] Lan zhiyong, Zhu jianlin, "Simulation reearch of three phase to three phase sparse matrix converter," *natural science journal of xiangtan university*, 2010,27(3):110-115.

[4]   CASDEI, D; SERRA, G; TANI, A; ZARRI, L. "Matrix Converter Modulation Strategies: A New General Approach on Space-Vector Representation of the Switch State", *IEEE Trans. On Industrial Electronics*, Vol. 49,No. 2, April 2012.

[5]   CASDEI, D; SERRA, G; TANI, A. "The Use of Matrix Converters in Direct Torque Control of Induction Machines", *IEEE Trans. On Industrial Electronics*, Vol. 48, No. 6, December 2010.

[6]   Romeo Ortega, Nikita Barabanov & Gerardo Escobar Valderrama, "Direct Torque Control of Induction Motors: Stability Analysis and Performance Improvement", *IEEE transactions on automatic control*, Vol. 46, No. 8, August 2011.

[7]   TAKAHASHI, I; NOGUSHI, T. "A New Quick-Response and High-Efficiency Control Strategy of an Induction Motor", *IEEE Trans. Industry Applications*, Vol. 1A-22, pp 820-827, October 2006.

[8]   DEPENBROCK, M. "Direct Self-Control (DSC) of Inverter-Fed Induction Machine", *IEEE Trans. on Power Electronics*, Vol. 3, No 4, pp 420-429, October 2008.

[9]   LEE K B, BLAABGERG F, "improved direct torque control for sensorless matrix converter drives with constant switching frequency and torque ripple reduction", *international journal of control, automation and system*, 2012,4(1):113-123.

[10] C. Lascu, I. Boldea, and F. Blaabjerg, "Very-low-speed variable-structure control of sensorless induction machine drives without signal injection," *IEEE Trans. Ind. Appl.*, vol. 41, no. 2, pp.591-598, Mar./Apr. 2010.

[11] C. Lascu, I. Boldea, and F. Blaabjerg, "Direct torque control of sensorless induction motor drives: a sliding-mode approach," *IEEE Trans. Ind. Appl.*, vol. 40, no.2, pp.582-590, Mar/Apr. 2011.

[12] Z. Xu and M. F. Rahman, "Direct torque and flux regulation of an IPM synchronous motor drive using variable structure control approach," *IEEE Trans. Power Electron.*, vol.22, no. 6, pp.2487-2498, Nov. 2007.

[13] V. I. Utkin, "Sliding mode control design principles and applications to electric drives," *IEEE Trans. Ind.Electron.*, vol.40, no. 1, pp.23-36, Feb. 2009.

[14] C. Lascu and A. M. Traynadlowski, "Combining the principles of sliding mode, direct torque control, and space vector modulation in a high-performance sensorless AC drive," *IEEE Trans. Ind. Appl.*, vol.40, no. 1, pp. 170-177, Jan./Feb. 2011.

[15] A. Naassani, E. Monmasson, and J. P. Louis, "Synthesis of direct torque and rotor flux control algorithms by means of sliding-mode theory," *IEEE Trans. Ind.Electron.*, vol.52, no.3, pp. 785-799, June. 2011.